

## Electronic structure and magnetic properties of $\text{Gd}_x\text{La}_{1-x}\text{Ni}_5$ system

This article has been downloaded from IOPscience. Please scroll down to see the full text article.

2006 J. Phys.: Condens. Matter 18 4861

(<http://iopscience.iop.org/0953-8984/18/20/011>)

View [the table of contents for this issue](#), or go to the [journal homepage](#) for more

Download details:

IP Address: 129.252.86.83

The article was downloaded on 28/05/2010 at 11:00

Please note that [terms and conditions apply](#).

# Electronic structure and magnetic properties of $\text{Gd}_x\text{La}_{1-x}\text{Ni}_5$ system

E Burzo<sup>1,4</sup>, L Chioncel<sup>2,5</sup>, I Costina<sup>1</sup> and S G Chiuzbăian<sup>3</sup>

<sup>1</sup> Faculty of Physics, Babeş-Bolyai University, RO-400084 Cluj-Napoca, Romania

<sup>2</sup> Department of Physics, University of Oradea, RO-410087 Oradea, Romania

<sup>3</sup> Paul Scherrer Institut, CH-5232 Villigen PSI, Switzerland

E-mail: [burzo@phys.ubbcluj.ro](mailto:burzo@phys.ubbcluj.ro)

Received 6 February 2006, in final form 12 April 2006

Published 2 May 2006

Online at [stacks.iop.org/JPhysCM/18/4861](http://stacks.iop.org/JPhysCM/18/4861)

## Abstract

Magnetic measurements were performed on  $\text{Gd}_x\text{La}_{1-x}\text{Ni}_5$  compounds in the temperature range 1.7–300 K and fields up to 90 kOe. There is a transition from a spin fluctuation behaviour, characteristic for  $\text{LaNi}_5$ , to a ferrimagnetic type ordering for  $x \geq 0.2$ . The critical field for appearance of induced Ni moment was estimated. Then, the nickel moments, at 1.7 K, increase linearly with the exchange field. Band structure calculations were performed on  $\text{RNi}_5$  and  $\text{Gd}_x\text{La}_{1-x}\text{Ni}_5$  systems. The Gd 5d band polarization is due to both local 4f–5d exchange and 5d–3d short range interactions with neighbouring atoms. There are also 5d–5d interactions through orbitals having lobes oriented along the *c*-axis. The differences between magnetic moments at 2c and 3g sites, obtained from band structure calculations, were correlated with their local environments. The mean effective nickel moments decrease when increasing gadolinium content, an opposite behaviour to that evidenced for ordered Ni moments at 1.7 K. This behaviour was attributed to gradual quenching of spin fluctuations by internal field.

(Some figures in this article are in colour only in the electronic version)

## 1. Introduction

The transition metal atoms (A) in rare-earth (R) or yttrium compounds show a wide variety of magnetic behaviours. As functions of crystal structure and composition, these cover the situations in which A atoms show a well defined magnetism or are in nonmagnetic state, crossing the region of onset or collapse of magnetism [1]. The transition from nonmagnetic

<sup>4</sup> Author to whom any correspondence should be addressed.

<sup>5</sup> Present address: Institute for Theoretical Physics and Computational Physics, Graz University of Technology, A-8010 Graz, Austria.

to magnetic state was analysed mainly in cobalt compounds, by using the molecular field approximation. For this purpose, the exchange field acting on cobalt was computed by using the phenomenological constants describing the exchange interactions between and inside the magnetic sublattices. It was suggested that an induced Co moment will occur above a critical field of the order of 0.7 MOe. Then, the cobalt moments vary linearly with exchange field and finally saturate [2]. The analysis of magnetic behaviour of some R–Co and R–Co–B systems confirmed the above model [3–5]. Small changes in cobalt moments were also evidenced for internal fields smaller than the critical one.

Little information was obtained on the magnetic behaviour of nickel in rare-earth compounds. In earlier studies on  $\text{RNi}_5$  systems, it was reported that nickel is not magnetic [1]. Analysing the magnetic properties of  $\text{Gd}_x\text{Y}_{1-x}\text{Ni}_5$  compounds [6] has shown that nickel 3d band is polarized in  $\text{GdNi}_5$ , and the mean nickel moment,  $M_{\text{Ni}}$  is  $0.16 \mu_{\text{B}}$ /atom. The  $M_{\text{Ni}}$  values decrease gradually as gadolinium is substituted by yttrium.  $\text{YNi}_5$  shows, at low temperatures, a Pauli-type paramagnetism.

In order to obtain information for nickel transition from nonmagnetic to magnetic state, we investigated  $\text{Gd}_x\text{La}_{1-x}\text{Ni}_5$  compounds. For this purpose, we analyse the exchange interactions in the above system, as well as in  $\text{RNi}_5$  compounds where R is a heavy rare-earth. In R–A type compounds the interactions are rather complicated and some models have been developed in order to describe the parallel alignment of magnetic moments for light rare-earths and transition metal ones and antiparallel in the case of heavy rare-earths. In earlier reports, the magnetic interactions between R and A atoms have been assumed to be of RKKY type [7]. Some works have been done in order to reverse the magnetic coupling by changing the electron concentrations and distances between magnetic atoms [8]. No effects on the magnetic coupling have been reported. Campbell [9] proposed a phenomenological model in which the 4f electrons of the rare-earth polarize their 5d band by local interactions and there are short-range 5d–3d interactions with neighbouring transition metal atoms. The existence of magnetic polarization of the 5d(4d) electron shell in rare-earth (yttrium)–transition metal compounds was evidenced by NMR [10], neutron diffraction [11] or magnetic circular x-ray dichroism [12]. The Campbell and RKKY models describe two extreme types of interactions. The first one takes into account short-range exchange interactions while the second one is of long range and oscillatory. The antiparallel coupling between 4f and 3d spins can be well described in terms of 3d–5d hybridization [13]. The degree of hybridization depends on the overlap matrix elements and on the energy separation between the 3d and 5d bands. If the energy separation is increasing the mixing decreases and the opposite holds when the separation decreases. The hybridization and the spin transfer are greater for the spin-down bands and there is an antiparallel coupling of A 3d and R 5d moments. Band structure calculations are an important tool to investigate the magnetic properties of  $\text{RA}_x$  compounds. By using this method the 3d–5d hybridization and spin transfer to the 5d band in  $\text{LuFe}_2$  was analysed [14]. Then, in compounds with magnetic rare-earths, the 4f–5d exchange interactions were described by the Hamiltonian  $\mathcal{H}_{4f-5d} = -2J_{4f-5d}S_{4f}S_{5d}$ , where  $J_{4f-5d}$  depends upon the 4f–5d overlap densities and is positive [13, 15]. According to Li *et al* [16], in addition to the  $J_{4f-5d}$  exchange integral, there are also exchange interactions of the 4f shell with p and s electrons described by  $J_{4f-5d}$  and  $J_{4f-6p}$ . All the exchange integrals decrease across the lanthanide series, but  $J_{4f-5d}$  dominates. Fähnle *et al* [17] showed that the intersublattice exchange parameter is determined mainly by the  $J_{4f-5d}$  and there is no major contribution from  $J_{3d-5d}$ . A review on band structure calculations performed for rare-earth–transition metal compounds was published [18]. Magnetic properties of  $\text{ACo}_5$  type compounds were particularly analysed.

In order to obtain more information on the magnetic couplings in  $\text{RA}_5$ -based compounds, in addition to magnetic measurements, band structure calculations and XPS measurements

were also performed. The 4f–5d and 5d–3d exchange interactions were analysed. The 5d band polarization was shown to be determined by both 4f–5d local exchange and 5d–3d hybridization, respectively. The band structure analysis in terms of projections of the bands onto orthogonal orbitals [19] allowed us to evidence the contributions of various orbitals to exchange interactions in  $RNi_5$  ( $R = La, Gd$ ) compounds. The exchange interactions between nickel atoms were also determined. In the light of the above data, the magnetic properties of the  $Gd_xLa_{1-x}Ni_5$  system were analysed. Some preliminary results have already been reported [20].

## 2. Experimental and computing methods

The  $Gd_xLa_{1-x}Ni_5$  compounds were prepared by the levitation method. The samples were thermally treated in vacuum at 1000 °C for one week. The x-ray diffraction analyses show the presence of only one phase having a hexagonal  $CaCu_5$ -type structure. In this structure, the R ( $R = Gd, La$ ) atoms occupy  $1a$  sites and Ni atoms are located in  $2c$  and  $3g$  positions. The lattice parameters are nearly linearly dependent on composition.

The magnetic measurements were performed in the temperature range 1.7–300 K and fields up to 90 kOe. The spontaneous magnetizations,  $M_s$ , were determined from magnetization isotherms, according to the approach to the saturation law:  $M_m = M_s(1 - a/H) + \chi_0 H$ . By  $a$  is denoted the coefficient of magnetic hardness,  $M_m$  is the measured magnetization in a field  $H$  and  $\chi_0$  is a field independent susceptibility. Above the Curie points, the susceptibilities,  $\chi$ , were determined from their field dependencies, according to a Honda–Arrott plot [21],  $\chi_m = \chi + cM_s H^{-1}$ , by extrapolating the measured values  $\chi_m$  to  $H^{-1} \rightarrow 0$ . By  $c$  is denoted a presumed magnetic ordered impurity content and  $M_s$  is their saturation magnetization. By this method any possible alteration of magnetic susceptibilities, as a result of the presence of magnetic ordered phase, is avoided. Generally, no magnetic ordered phases, above  $T_c$ , were observed. If they exist, these are smaller than 0.1 mol%.

Band structure calculations were carried out by using the *ab initio* tight binding linear muffin tin orbital method in the atomic sphere approximation. The detailed procedure of calculation was described elsewhere [19, 22–24]. In the framework of the local density approximation (LDA) the total electronic potential is the sum of external, Coulomb and exchange–correlation potentials [25]. The functional form of the exchange–correlation energy used in the present work was the free electron gas parametrization of Von Barth and Hedin [26]. Relativistic correlations were included. A  $Gd_3Ni_{15}$  superstructure having three times greater unit cell than that of  $GdNi_5$  was assumed. In this cell, the Gd was substituted by one, two or three lanthanum atoms, corresponding to compositions  $x = 0.67, 0.33$  and 0. The band structure and the bonding were analysed in terms of projections of the bands onto orthogonal orbitals.

## 3. Band structure calculations

Band structure calculations were performed on  $RNi_5$  heavy rare-earth compounds as well as on the  $Gd_xLa_{1-x}Ni_5$  system. The dependence of Ni( $2c$ ) and Ni( $3g$ ) magnetic moments as a function of De Gennes factor,  $G = (g_J - 1)^2 J(J + 1)$ , in  $RNi_5$  compounds with heavy rare-earths is plotted in figure 1. The computed transition metal moments are linearly dependent on  $G$ ,  $M_{Ni} = M_{Ni}(0) + \alpha G$ . The slope of this variation is  $1.6 \times 10^{-3} \mu_B$ . Since the Ni magnetic moments are rather small, no possibility to have an accurate experimental determination by neutron diffraction studies was shown. The experimental errors are of the order of magnitude of Ni moments. For example, in  $TbNi_5$ , a value  $M_{Ni} = 0.0 \pm 0.2 \mu_B/\text{atom}$  was reported [27].

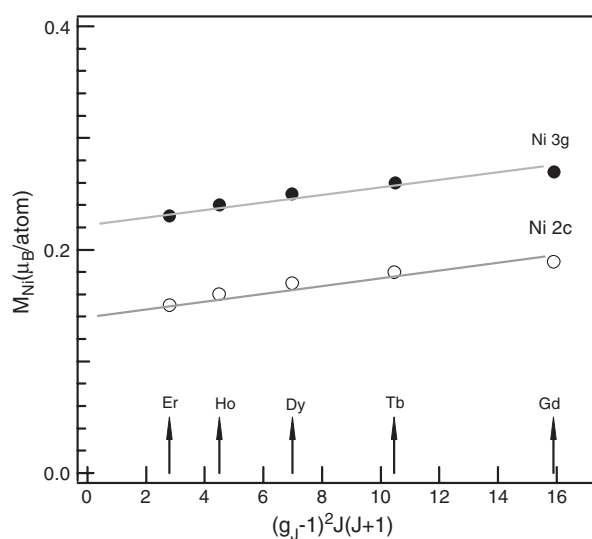


**Figure 1.** Dependences of the magnetic moment of Ni, at 2c and 3g sites, in  $RNi_5$  compounds with heavy rare-earths, as a function of De Gennes factor.

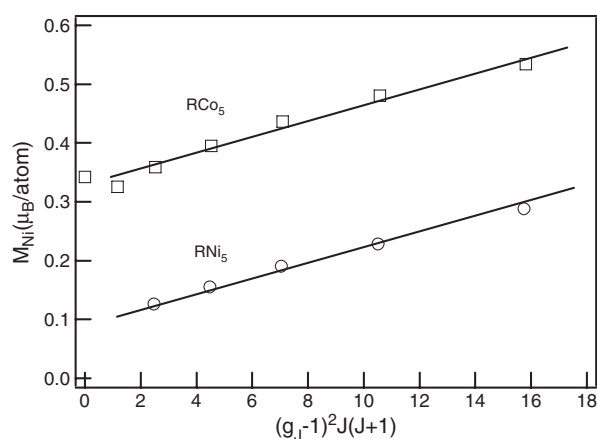


**Figure 2.** The 5d band polarizations in  $RA_5$  ( $A = Co, Ni$ ) compounds with heavy rare-earths, as a function of De Gennes factor.

The R 5d band polarizations,  $M_{5d}$ , in  $RNi_5$  and  $RCo_5$  [28] are also linearly dependent on De Gennes factor—figure 2.

$$M_{5d} = M_{5d}(0) + \beta G. \quad (1)$$

The slopes,  $\beta = 1.4 \times 10^{-2} \mu_B$ , are not dependent on A partner. The contributions to polarizations,  $M_{5d}(0)$ , are  $0.32 \mu_B$  for  $A = Co$  and  $0.08 \mu_B$  for  $A = Ni$ .

The analysis of  $M_{5d}$  polarizations suggests the presence of two contributions. The first one is due to local 4f–5d exchange and is the same for a given R element. The second one,  $M_{5d}(0)$ , is dependent on the magnetic contribution of A partner and can be attributed to 5d–3d hybridization. As we have shown already [28], this contribution to 5d polarization increases linearly with A magnetic contributions. For example, in  $GdCo_5$  and  $GdNi_5$  compounds, the

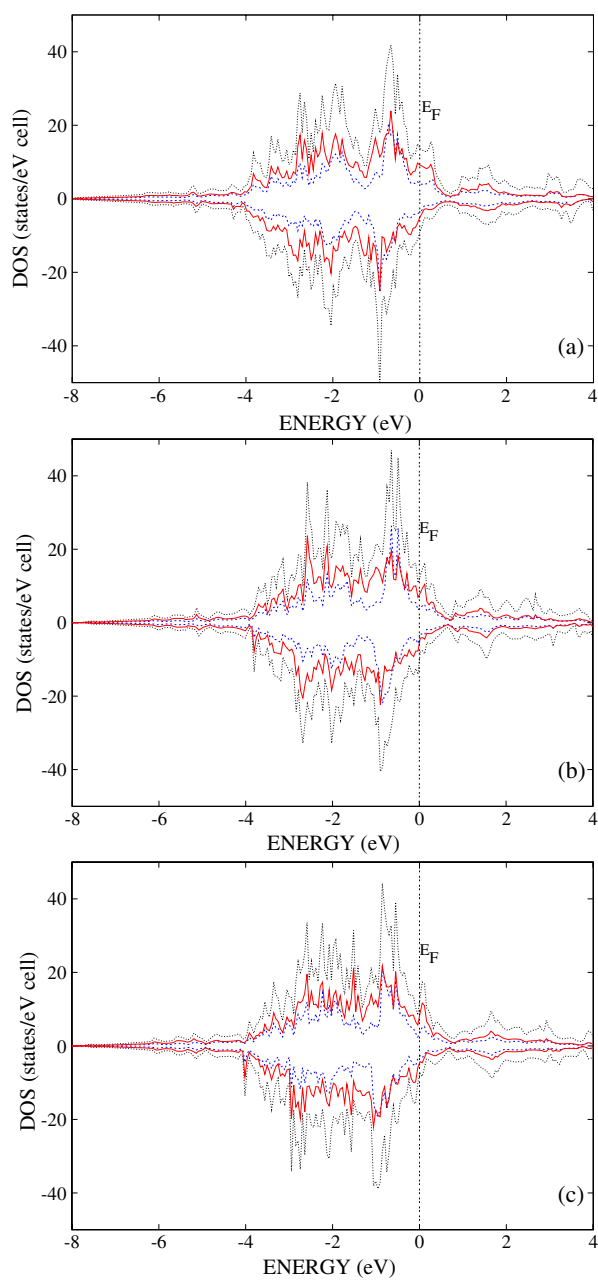


**Figure 3.**  $Gd_3Ni_{15}$  (a);  $Gd_2LaNi_{15}$  (b);  $GdLa_2Ni_{15}$  (c): densities of states for Ni(2c) (dashed line), Ni(3g) (thin solid line) and total densities of states (dotted line).

4f–5d contributions to 5d polarizations are identical,  $\approx 0.20 \mu_B$ , and those induced by 5d–3d exchange interactions are of 0.32 and  $0.08 \mu_B$  respectively.

The total densities of states as well as the partial DOS Ni(2c) and Ni(3g) projected bands for  $Gd_xLa_{1-x}Ni_5$  compounds with  $x = 1.0, 0.67$  and  $0.33$  are plotted in figure 3. A gradual increase of the exchange splitting both at Ni(2c) and Ni(3g) sites was evidenced

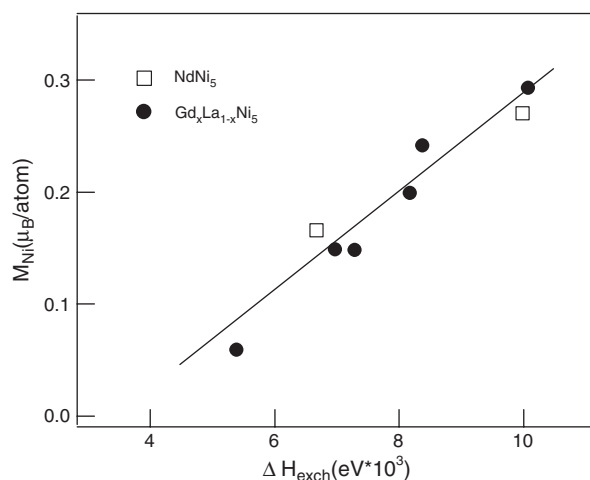


**Figure 4.** The correlation between Ni magnetic moments at 2c and 3g sites and exchange splitting of their 3d bands.

**Table 1.** Data obtained from band structure calculations.

Compounds	Magnetic moments ( $\mu_B/\text{atom}$ )					
	Gd 4f	Gd 5d	La 5d	Ni(2c)	Ni(3g)	$\langle \text{Ni} \rangle$
GdNi <sub>5</sub>	−7	−0.275	—	0.199	0.293	0.255
Gd <sub>2</sub> LaNi <sub>15</sub>	−7	−0.249	−0.056	0.149	0.242	0.205
GdLa <sub>2</sub> Ni <sub>15</sub>	−7	−0.230	−0.032	0.082	0.145	0.120

when increasing gadolinium content. The computed magnetic moments, at various Ni sites, as well as Gd 5d band polarization decrease when increasing La content—table 1. In addition, a polarization of La 5d band is induced in magnetic ordered compounds. The Gd 5d and La 5d band polarizations are parallel to Gd 4f moments and antiparallel to Ni ones, respectively.

The computed magnetic moments at Ni(3g) sites are higher than those of 2c sites. This behaviour may be attributed to different local environments. The 2c site in GdNi<sub>5</sub> has six Ni(3g) and three Ni(2c) atoms as well as three Gd ones, while the 3g sites have four Ni(2c), four Ni(3g) and four Gd as nearest neighbours. The strength of exchange interactions between nickel atoms and gadolinium ones are more important than between nickel atoms. The nickel moments are essentially induced by the exchange interactions due to the presence of gadolinium. Thus, the exchange splitting of the Ni(2c) 3d band is greater than for Ni(3g) sites because of the higher number of Gd nearest neighbours. In figure 4 we plotted the correlation between Ni moments at 2c and 3g sites and exchange splitting of their 3d bands. The data obtained in the case of the NdNi<sub>5</sub> system are also plotted [29]. There seems to be a critical value of the exchange splitting for which a Ni moment will appear, of the order of  $\sim 0.0030$  eV. Then a linear relation between Ni moments and the exchange splittings of their 3d bands is shown.

The band structure calculations show that at low temperatures LaNi<sub>5</sub> is a Pauli-type paramagnet. The computed magnetic susceptibility, at 0 K, from density of states,  $N$ , at the Fermi level is  $1.88 \times 10^{-3}$  emu/f.u. [30]. We also determined the  $N'$  and  $N''$ , the first and second derivatives of the density of states at the Fermi level, and thus the temperature dependence of the magnetic susceptibility, at the low temperatures described by

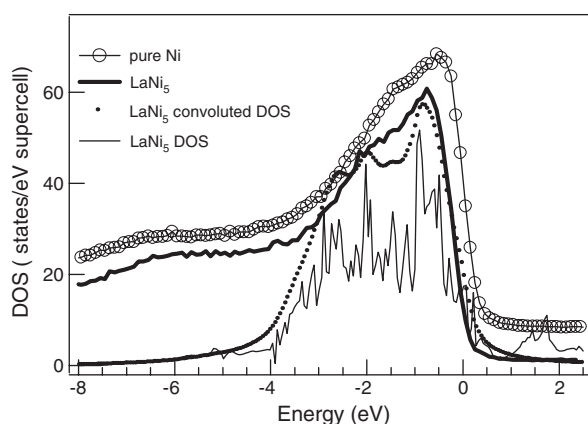


**Figure 5.** Comparison of the measured XPS valence band (thick solid line) and convoluted DOS (by Lorentzians of half width of 0.4 eV taking into account proper cross sections for partial bands with different  $l$  symmetry; dashed line) for  $LaNi_5$ . The XPS spectrum of Ni is also plotted.

the relation  $\chi = \chi_0(1 + dT^2)$ , where the expression of  $d$  was given by Beal-Monod [31]  $d = (\pi^2/6)(2(N''/N) - 1.2(N^2/N^2))s^2$  where  $s$  is the Stoner exchange enhancement factor. A value of  $d = 1.22 \times 10^{-3} K^{-2}$  was theoretically computed.

A comparison of the computed density of states for  $LaNi_5$  and the measured XPS valence band spectra for  $LaNi_5$  and Ni are plotted in figure 5. The computed density of states describe rather well the  $LaNi_5$  XPS spectrum. There is also a similarity of the Ni 3d band for pure Ni and that of  $LaNi_5$ . This fact evidences that the valence band of  $LaNi_5$  is mainly derived from the Ni 3d one. The structure at about 6 eV binding energy in the XPS spectrum is the well known Ni satellite [30]. The contribution of La states to the valence band of  $LaNi_5$  is not visible in the XPS spectrum because of the low cross section of lanthanum. In addition, the contribution of La to DOS is very weak.

The band structures and bonding in  $LaNi_5$  and  $GdNi_5$  were analysed in terms of projections of the bands onto orthogonal orbitals. The Brillouin zone of hexagonal  $RNi_5$ -type structure is described by vectors:  $b_1 = (4\pi/(a\sqrt{3}), 0, 0)$ ,  $b_2 = (2\pi/(a\sqrt{3}), (2\pi/a), 0, 0)$ ,  $b_3 = (0, 0, (2\pi/c))$  [32]. In figure 6 the band structures are projected onto the orthogonal LMTOs [19], or equivalently, partial waves normalized to unity in their respective spheres. The zero of the energy is taken at the Fermi level. In such a 'fat' band structure, each band is given a width proportional to the (sum of the) corresponding orthonormal orbital(s). In figure 6, 100% for  $LaNi_5$  and  $GdNi_5$  corresponds to 1/30 the size of the energy axis, that is, to 0.4 eV. A local system of coordinates was used for Ni(2c), Ni(3g) and Gd(1a) in which the  $z$ -axis was parallel to the  $c$ -axis for all sites. For Ni(2c) the  $x$ -axis was along the shortest Ni(2c)–Ni(2c) distance. For Ni(3g) the  $y$ -axis was parallel to  $a$ -axis. In the case of the La site in  $LaNi_5$ , the dominant 5d–5d hybridizations are between orbitals with lobes pointed along the  $c$ -axis, which leads to decorated (fat) bands. The bands are strongly dispersed in  $K$ – $\Gamma$  and  $\Gamma$ – $A$  directions. Important interactions are between almost all the projected orbitals of nickel. As an example for the Ni(2c) site in  $LaNi_5$ ,  $d_{xy}$  orbitals create 'fat' bands at  $-1$  eV. In  $GdNi_5$ ,  $d_{xz}(\downarrow)$  orbitals create a 'fat' band near the Fermi level and  $d_{xz}(\uparrow)$  create 'fat' bands at  $\approx 0.5$  eV above the Fermi level. In the case of the Ni(3g) site in  $LaNi_5$ , 'fat' bands in particular are formed at the Fermi level for  $d_{3z^2-1}$  orbitals along the  $A$ – $L$  direction and  $d_{x^2-y^2}$  orbitals along the  $\Gamma$ – $A$  direction. In  $GdNi_5$  'fat' bands are created at the Fermi level for  $d_{3z^2-1}(\downarrow)$  orbitals along the  $A$ – $L$  direction and  $d_{x^2-y^2}(\downarrow)$  orbitals along the  $\Gamma$ – $A$  direction. At 0.4 eV above the Fermi level, 'fat' bands are



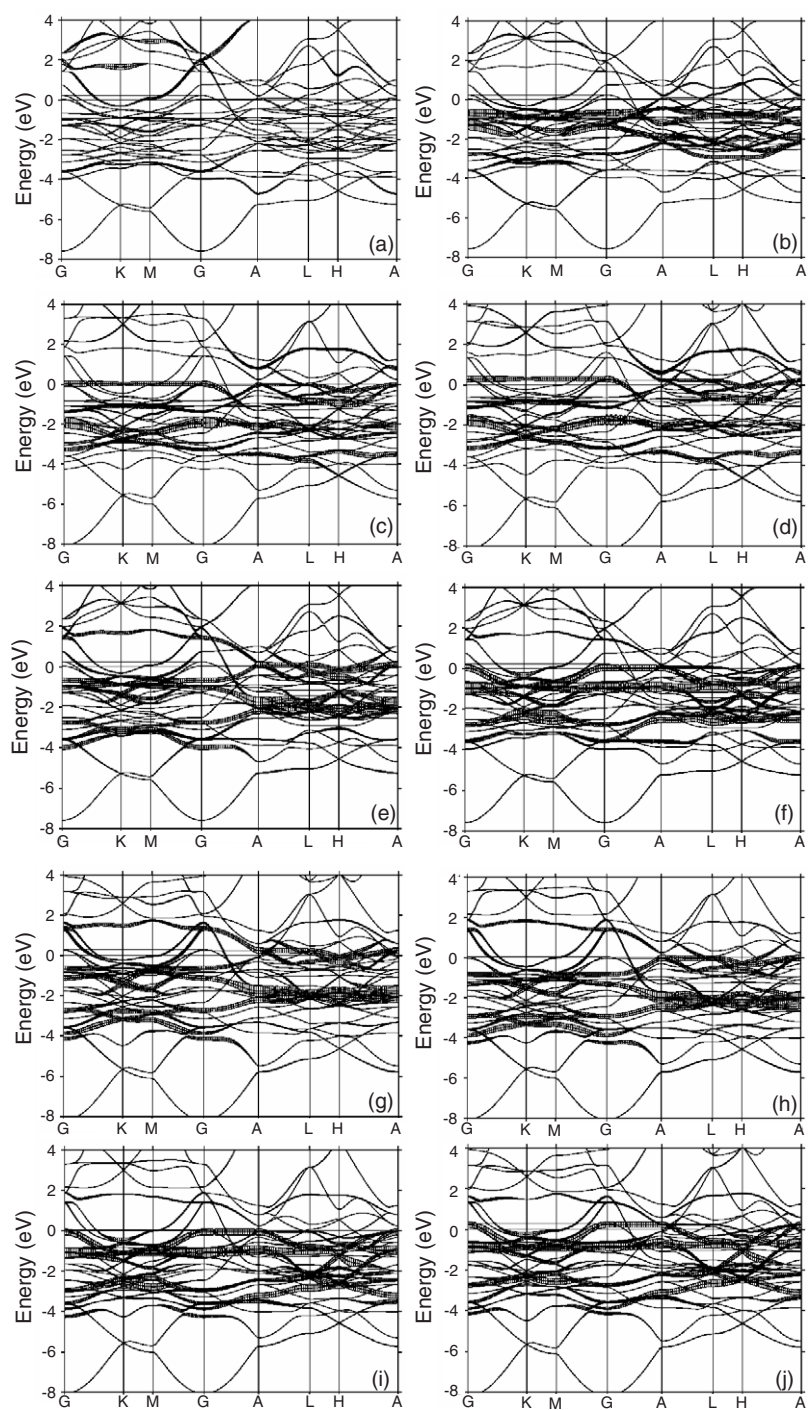


**Figure 6.** Energy bands of LaNi<sub>5</sub> and GdNi<sub>5</sub> decorated with orthogonal orbital character: (a) La 5d<sub>3z<sup>2</sup>-1</sub>, (b) Ni(2c) in LaNi<sub>5</sub> (d<sub>xy</sub>); (c), (d) Ni(2c) in GdNi<sub>5</sub> (d<sub>xz</sub> ↑) and (d<sub>xz</sub> ↓); (e) Ni(3g) in LaNi<sub>5</sub> d<sub>3z<sup>2</sup>-1</sub>; (f) Ni(3g) in LaNi<sub>5</sub> d<sub>x<sup>2</sup>-y<sup>2</sup></sub>; (g), (h) Ni(3g) in GdNi<sub>5</sub> d<sub>3z<sup>2</sup>-1</sub> ↓ d<sub>3z<sup>2</sup>-1</sub> ↑; (i), (j) Ni(3g) in GdNi<sub>5</sub> d<sub>x<sup>2</sup>-y<sup>2</sup></sub> ↓ and GdNi<sub>5</sub> d<sub>x<sup>2</sup>-y<sup>2</sup></sub> ↑.

formed by  $d_{3z^2-1}(\uparrow)$  orbitals along the  $A-L$  direction and  $d_{x^2-y^2}(\uparrow)$  orbitals along the  $\Gamma-A$  direction.

The exchange interactions between nickel atoms were also computed by using a recently developed approach [33]. Using the Green function method to calculate the effective exchange interaction parameter,  $J_{ij}$ , as a second derivative of the ground state energy with respect to the magnetic rotation angle [34], it was shown that the exchange interactions between  $i$  and  $j$  atoms may be described by [33]

$$J_{ij} = \sum_{\{m\}} I_{mm'}^i \chi_{mm'm''m'''}^{ij} I_{m''m'''}^j \quad (2)$$

where the spin dependent potentials,  $I^i$ , are expressed in terms of the single particle potential  $V_{mm'}$ :  $I_{mm'}^i = V_{mm'}^{i\uparrow} - V_{mm'}^{i\downarrow}$ , while the effective inter-sublattice susceptibilities,  $\chi^{ij}$ , were defined in terms of the LDA eigenfunctions as

$$\chi_{mm'm''m'''}^{ij} = \sum_{knn'} \frac{n_{nk\uparrow} - n_{n'k\downarrow}}{\varepsilon_{nk\uparrow} - \varepsilon_{n'k\downarrow}} \Psi_{nk\uparrow}^{ilm^*} \Psi_{nk\uparrow}^{ilm''} \Psi_{n'k\downarrow}^{ilm'} \Psi_{n'k\downarrow}^{jlm^*}. \quad (3)$$

We denoted by  $n_i$  the orbital occupancy of d electrons,  $l$  the orbital quantum number and  $m$  the magnetic quantum number. By using the above relations we obtained the exchange interactions between nickel atoms situated in first,  $J_{ij}(1)$ , and second,  $J_{ij}(2)$ , coordination shells. For GdNi<sub>5</sub>, values  $J_{3g-3g}(1) = 57$  K,  $J_{3g-3g}(2) = 28$  K,  $J_{2c-3g}(1) = 26$  K, and  $J_{2c-3g}(2) = 12$  K were determined. The exchange interactions between Ni(2c) and Ni(2c) are rather small. When randomly substituting Gd by La in CaCu<sub>5</sub>-type structure, the exchange interactions between nickel atoms decrease. This behaviour may be connected mainly with the diminution of nickel moments. There is also a difference between the values of the exchange interactions determined between the same types of nickel atoms situated near an R(1a) site occupied by Gd,  $J(\text{Gd})$ , and La,  $J(\text{La})$ , respectively. In figure 7 we have plotted a CaCu<sub>5</sub>-type structure where two Gd atoms were replaced by La, corresponding to GdLa<sub>2</sub>Ni<sub>5</sub> composition, and the positions of Ni atoms were numbered. The  $J_{3g-3g}(\text{La})$  values, between Ni atoms numbered according to figure 7, are 37 K (14–15), 18 K (14–16) and 11 K (15–16), while for  $J_{3g-3g}(\text{Gd})$  values 40 K (8–9), 23 K (8–12) and 17 K (9–12) were obtained. Similarly, for  $J_{2c-3g}(\text{La})$  values 23 K (4–14), 19 K (4–16) and 7 K (4–15) were obtained, smaller than  $J_{2c-3g}(\text{Gd})$  of 24 K (2–8), 21 K (2–12) and 9 K (2–9). We note that the exchange interactions thus obtained are in rather good agreement with those expected from the Curie temperatures experimentally determined and reported in the next section ( $T_c(\text{GdNi}_5) \cong 35$  K,  $T_c(\text{Gd}_{0.33}\text{La}_{0.67}\text{Ni}_5) \cong 23$  K).

### 3.1. Magnetic data

The thermal variations of spontaneous magnetizations for Gd<sub>x</sub>La<sub>1-x</sub>Ni<sub>5</sub> compounds with  $x \geq 0.2$  are plotted in figure 8. The magnetizations, at 1.7 K, decrease nearly linearly when increasing La content—figure 9. On the same figure the magnetizations obtained from band structure calculations are also given. There is a good agreement between experimentally determined and computed values per formula unit. The differences are smaller than  $0.3 \mu_B$ . The Curie temperatures decrease gradually from  $T_c = 35$  K ( $x = 0$ ) and finally the LaNi<sub>5</sub> is a paramagnet.

The saturation magnetizations, at 1.7 K, for compounds with  $x \geq 0.2$  are somewhat lower than the values expected in the supposition that only gadolinium has a magnetic moment. This suggests that nickel atoms have magnetic contributions which are anti-parallel oriented to the gadolinium moment. Assuming that the magnetic moment per gadolinium atom is  $\cong 7.24 \mu_B$ , as a mean value determined from band structure calculations, where Gd 5d polarization was

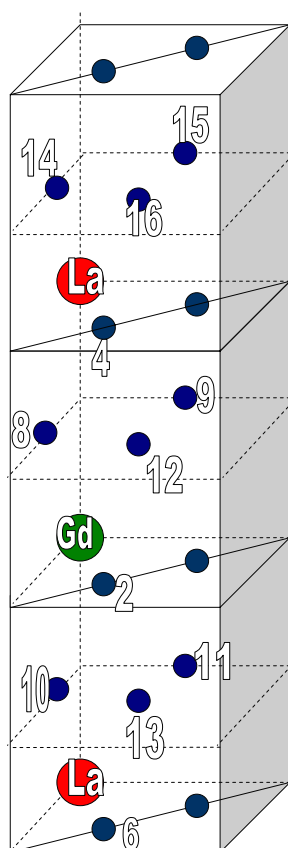


Figure 7.  $\text{CaCu}_5$ -type structure where two Gd atoms were substituted by La.

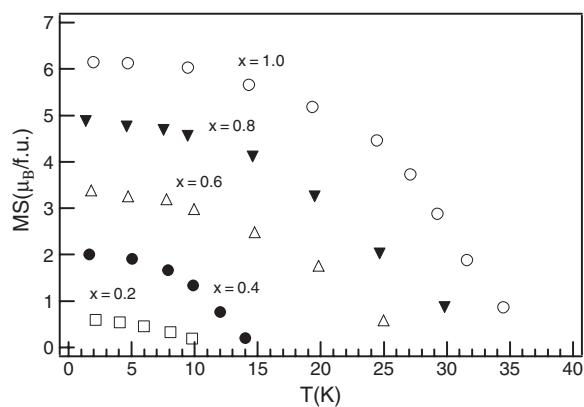
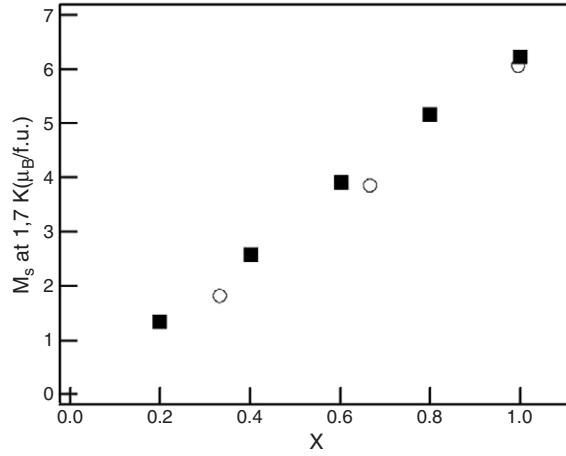
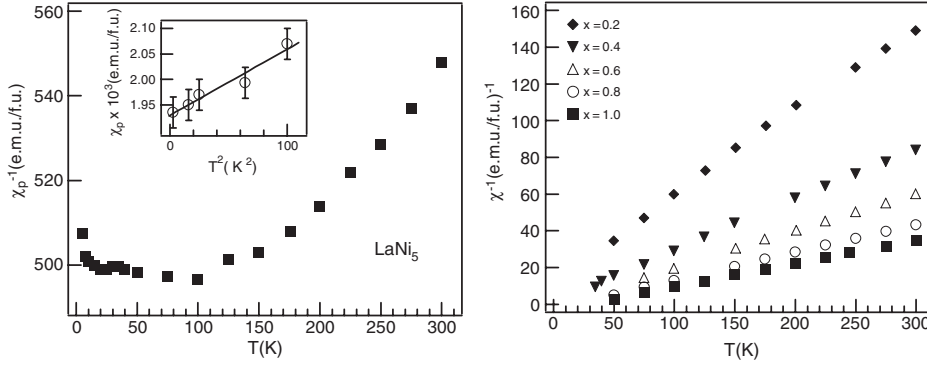


Figure 8. Thermal variations of spontaneous magnetizations in  $\text{Gd}_x\text{La}_{1-x}\text{Ni}_5$  system.

included, we determined the composition dependence of the mean Ni moments,  $M_{\text{Ni}}$ . These values decrease when increasing lanthanum content. We note that the mean nickel moments obtained from band structure calculations have the same trend as those determined from saturation measurements, but are higher by  $\approx 0.06 \mu_B$ .



**Figure 9.** Composition dependence of saturation magnetizations at 1.7 K. The data obtained from band structure calculation (o) are also plotted.



**Figure 10.** The thermal variations of reciprocal susceptibilities for  $\text{LaNi}_5$  (a) and  $\text{Gd}_x\text{La}_{1-x}\text{Ni}_5$  ( $x \leq 0.2$ ) (b). In the inset of (a) the  $T^2$  dependence of the susceptibilities at  $T \leq 10$  K is shown.

The superimposed susceptibilities,  $\chi_0$ , on the magnetization isotherms, at 1.7 K, are  $1.68 \times 10^{-2}$  emu/f.u. in  $\text{GdNi}_5$  and decrease gradually to  $1.38 \times 10^{-2}$  emu/f.u. ( $x = 0.8$ ),  $1.36 \times 10^{-2}$  emu/f.u. ( $x = 0.4$ ) and  $0.235 \times 10^{-2}$  emu/f.u. ( $x = 0.2$ ). The last value is close to that determined in  $\text{LaNi}_5$ , at 1.7 K—figure 10. These data show that the exchange enhancement factor of the electron conduction band increases by nearly one order of magnitude when increasing gadolinium content and exchange interactions, respectively.

The thermal variations of reciprocal susceptibilities are plotted in figure 10. In the case of  $\text{LaNi}_5$ , in the low temperature range ( $T \leq 10$  K), the susceptibilities follow a  $T^2$  dependence  $\chi = \chi(0)(1 + dT^2)$  with  $d = 1.3 \times 10^{-3} \text{ K}^{-2}$ , close to the  $d$  value obtained from band structure calculation. The magnetic susceptibility for  $\text{LaNi}_5$  increases and has a maximum at  $T = 90$  K. Above  $T^* \approx 150$  K, the reciprocal susceptibility follows a Curie–Weiss type behaviour  $\chi = C(T - \theta)^{-1}$ . The paramagnetic Curie temperature is negative,  $\theta = -1104$  K. From the Curie constant,  $C$ , an effective magnetic moment,  $M_{\text{eff}}(\text{Ni}) = 2.15 \mu_B/\text{atom}$ , was determined.

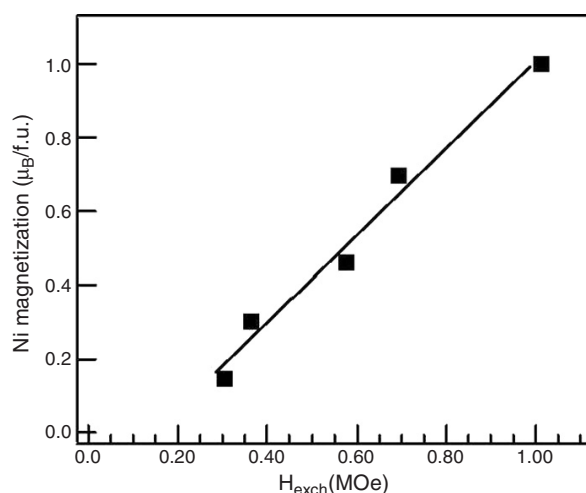


**Figure 11.** Dependence of Ni magnetizations at, 1.7 K, on exchange field.

The reciprocal susceptibilities for compounds with  $x \geq 0.2$  show nonlinear temperature dependences, typical for a ferrimagnetic system. The  $\chi$  values can be described by the relation [35]:  $\chi^{-1} = \chi_0^{-1} + TC^{-1} - \sigma(T - \theta)^{-1}$ , where  $\chi_0^{-1}$ ,  $\sigma$  and  $\theta$  are parameters related to molecular field coefficients characterizing the interactions inside and between Gd and Ni magnetic sublattices. This type of variation is more evident as the gadolinium content decreases. In the high temperature range, linear dependences were shown. According to the addition law of magnetic susceptibilities and supposing that the effective gadolinium moment is given by the free ion value [36], we determined the contributions of nickel atoms to the Curie constants and the  $M_{\text{eff}}(\text{Ni})$ , effective nickel moments, respectively. The  $M_{\text{eff}}(\text{Ni})$  values decrease rapidly in the composition range  $0 \leq x \leq 0.2$  from  $2.15 \mu_{\text{B}}/\text{atom}$  ( $x = 0.2$ ) and then nearly linearly when increasing gadolinium content. The behaviour is different from that evidenced for Ni magnetic moments at 1.7 K.

The paramagnetic Curie temperature,  $\theta$ , for  $\text{LaNi}_5$  is very high in absolute magnitude. The asymptotic temperatures, for composition  $x \geq 0.2$  determined by extrapolating the  $\chi^{-1}$  versus  $T$  from the high temperature range to  $\chi \rightarrow 0$ , decrease (in absolute magnitude) from  $\theta = -45 \text{ K}$  ( $x = 0.2$ ), become near nil for  $x = 0.6$  and are positive for higher gadolinium content.

From paramagnetic data, by considering a two sublattice ferrimagnet, in the molecular field approximation, we evaluated the  $N_{ij}$  ( $i, j = \text{Gd, Ni}$ ) exchange interaction parameters inside and between magnetic sublattices. The  $N_{\text{Gd-Ni}}$  values are approximately constant along series while the  $N_{\text{Ni-Ni}}$  ones increase when decreasing the Gd content. Starting from these parameters we evaluated the exchange field acting on nickel atoms. The nickel magnetizations, at 1.7 K, are linearly dependent on the exchange fields as seen in figure 11, showing that these are essentially induced. A critical value of the exchange field,  $H_{\text{exch}} \approx 0.3 \text{ MOe}$ , for the appearance of the Ni induced moment, is suggested. In this field, the Ni moment is near nil,  $M_{\text{Ni}} \approx 0.03 \mu_{\text{B}}/\text{atom}$ , of the order of magnitude of experimental errors.

These data suggest that the interactions involving gadolinium atoms increase gradually with  $x$  and dominate for the composition range  $x \geq 0.6$ . On the other hand, in the composition range  $0 \leq x \leq 0.2$ , there seems to be a change in the dominant magnetic behaviour and the appearance of induced Ni moment.

#### 4. Discussion

The band structure calculations show that when increasing the magnetic contributions of transition metals, for a given type of structure, in compounds with similar rare-earths, the R 5d band polarization is translated to higher values although the same slope, as function of De Gennes factor, is observed. Thus, the composition dependence of 5d band polarization, described by the relation (1), suggests the presence of two contributions. The first one,  $\alpha G$ , is related to the local 4f–5d exchange interactions and seems to be essentially determined by rare-earth moment. The second one,  $M_{5d}(0)$ , can be attributed to the induced polarization by short-range 5d–3d and 5d–5d exchange interactions. The  $M_{5d}(0)$  values may be identified by extrapolation of  $M_{5d}$  versus  $G$  variation to  $G = 0$ . The dominant contribution to  $M_{5d}(0)$  is given by the exchange interactions of R 5d with neighbouring transition metal atoms. A small contribution is also expected from R 5d–R 5d exchange interactions, which takes place mainly through orbitals with lobes oriented along the  $c$ -axis. Thus, the short range exchange interactions may be described by the Hamiltonian

$$\mathcal{H} = -2 \sum_i J_{3d_i-5d} S_{5d} \sum_{n_i} S_{3d_i n_i} - 2 J_{5d-5d} S_{5d} \sum_j S_{5d_j}. \quad (4)$$

We denoted by  $i$  the number of 3d atoms situated in the first coordination shell to an R atom;  $n_i$  is the number of atoms occupying a given  $i$  site,  $j$  is the number of R nearest neighbour atoms to a given R site and  $S$  the corresponding spin values.

The 5d–3d and 5d–5d exchange interactions act as an internal field,  $H_{\text{exch}}$ , on the 5d band and induce an additional polarization to that given by the local 4f–5d exchange. In the molecular field approximation the exchange field may be written as  $H_{\text{exch}} = N_{5d-3d} M_{3d} + N_{5d-5d} M_{5d}$ , where  $N_{5d-3d}$  and  $N_{5d-5d}$  are the molecular field coefficients describing the R 5d–M 3d and R 5d–R 5d exchange interactions, respectively. In  $RCO_5$  or in related  $RCO_4B$  compounds, the contribution of the second term in relation (4) may be neglected since  $S_{3d} \ll S_{5d}$ . For  $RNi_5$  compounds the 5d band polarization is of the order of Ni 3d moments and consequently this term cannot be neglected. In this case we consider  $N_{5d-3d} \cong N_{5d-5d}$ . We showed that the exchange interactions between Ni atoms are of the same order of magnitude as the Curie temperatures, which are expected to be determined mainly by gadolinium–nickel exchange interactions. Consequently, this approximation seems to be reasonable.

As a result of the above discussion it results that the exchange field is proportional to total d magnetization,  $M_d = M_{3d} + M_{5d}$ , namely  $H_{\text{exch}} = \xi M_d$ . Previously [37], we showed that the induced 3d band polarization in rare-earth transition metal compounds, above the critical field for appearance of 3d magnetic moment, is proportional to the exchange field  $\Delta M_d \propto H_{\text{exch}}$ . Thus, finally we have  $M_{5d}(0) = \gamma M_d$ . According to the above relation, as well as the Hamiltonian for complex crystal structures (see equation (4)), where R atoms have different local environments as in  $RCO_4B$  type structures, the  $M_{5d}$  band polarization will be proportional to the  $\sum n_k M_k$  where  $n_k$  is the number of R and A atoms situated in the first coordination shell having  $M_k$  magnetic moments. The  $M_{5d}(0)$  values are plotted in figure 12 as a function of  $\sum n_k M_k$ . In addition to data obtained for  $RNi_5$  and  $RCO_5$  based compounds, the 5d band polarization  $M_{5d}(0)$  for R(1a) and R(1b) sites in  $RCO_4B$  compounds are also given. As seen in figure 12, there is a linear dependence of  $M_{5d}(0)$  on  $\sum n_k M_k$  in agreement with the above discussion.

According to the above relation we computed the induced R 5d polarization due to 5d–3d exchange interactions, by using the Ni moments determined from band structure calculations—table 1. Values  $M_{5d}(0) = 0.07, 0.05$  and  $0.035 \mu_B$  for  $Gd_xLa_{1-x}Ni_5$  with  $x = 1.0; 0.67$  and  $0.33$  were obtained. The total 5d band polarizations for the above compositions, admitting that

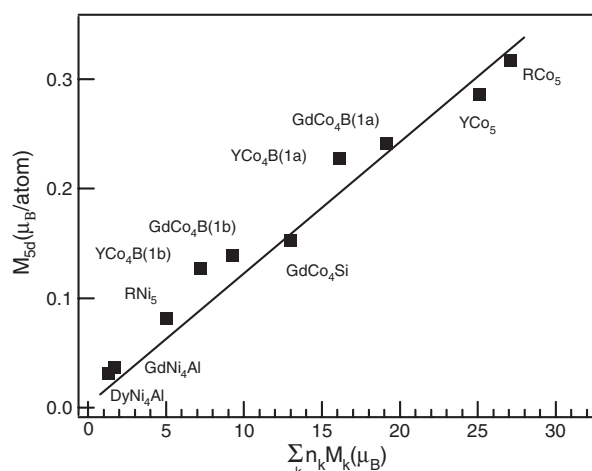


**Figure 12.** The  $M_{5d}(0)$  contributions to 5d band polarization due to 5d–3d short range exchange interactions as a function of  $\sum_k n_k M_k$ .

the 4f–5d contribution is  $\approx 0.20 \mu_B$  as shown in section 3, are  $0.27 \mu_B$ ,  $0.25 \mu_B$  and  $0.235 \mu_B$ , respectively, in agreement with those obtained from band structure calculations—table 1.

There is also an induced polarization on the La 5d band. This is a result of La 5d–Ni 3d and La 5d–Gd 5d exchange interactions. The La 5d band hybridizes with Ni 3d bands of nearest neighbouring Ni atoms. In addition, there are also La 5d–Gd 5d interactions through the orbitals with lobes oriented along the *c*-axis, as evidenced from band structure calculations. Considering the above paths of interactions and supposing, as above, that  $M_{5d}(0)$  is proportional to the magnetization of nearest neighbouring atoms, we determined values  $M_{5d}(0) = 0.057 \mu_B$  ( $x = 0.67$ ) and  $0.039 \mu_B$  ( $x = 0.33$ ), in agreement with computed data—table 1. The Ni 3d–Ni 3d exchange interactions involve almost all projected orbitals, as evidenced already by the presence of ‘fat’ bands. The strengths of the interactions between Ni atoms were evaluated in section 3. The greater values were shown between Ni(3g)–Ni(3g). The computed values of the exchange interactions between Ni atoms decrease when Gd is substituted by La and are of the order of magnitude of those estimated from Curie temperatures. Since gadolinium and lanthanum are isoelectronic, no band filling mechanism is present when changing the composition.

The La substitution by Gd leads to variations of the exchange interactions and consequently to different exchange splitting of Ni 3d bands when increasing gadolinium content. The fact that the nickel moments change linearly with exchange fields suggests that mean  $M_{Ni}$  values are essentially induced. We evaluated the mean exchange fields acting on nickel atoms. Above a critical field of  $\approx 0.3$  MOe the mean  $M_{Ni}$  values determined at 1.7 K increase linearly with the exchange field  $M_{Ni} = \gamma H_{\text{exch}}$  with  $\gamma = 0.9 \mu_B/\text{MOe}$ —figure 11. The nickel moments seem to be more sensitive to exchange interactions as compared to cobalt ones, where a value  $\gamma = 0.3 \mu_B/\text{MOe}$  was previously obtained [2, 37].

Above a value of the exchange splitting,  $\Delta E_{\text{exch}} \approx 5 \times 10^{-3}$  eV, there is a linear correlation between the Ni moments and their band splittings—figure 4. In addition, the mean nickel moments, at 1.7 K, increase linearly with the exchange field—figure 11. In spite of the fact that the data from figure 11 refer to mean nickel moments and in figure 4 on their distinct values for 2c and 3g sites, the above trends suggest that Ni 3d band splitting is linearly dependent on the



exchange field. The critical exchange splitting  $\approx 3 \times 10^{-3}$  eV, for the appearance of induced Ni moment, corresponds to an exchange field of  $\approx 0.5$  MOe. A value of critical exchange field of  $\approx 0.3$  MOe has been suggested from magnetic measurements, somewhat smaller than that estimated from band structure calculations. The difference may be attributed to the fact that in the first case we used the values of local moments and in the other one the mean Ni moments. Also, the molecular field coefficients, used in determining the exchange field, were obtained from paramagnetic data. Since the moments for Ni, at 1.7 K, and the values deduced from Curie constants are different, this analysis can influence the values of exchange interaction parameters. In spite of the above approximations the estimated critical fields from the two different sets of data are in reasonable agreement.

The magnetic susceptibilities for  $\text{LaNi}_5$ , at low temperatures ( $T \leq 10$  K), follow a relation of the form  $\chi = \chi_0(1 + dT^2)$ , typical for a Pauli-type paramagnetic system. The  $d$  value obtained from band structure calculation agrees well with that experimentally determined. As mentioned, above  $T^* \approx 150$  K, the reciprocal susceptibilities follow a Curie–Weiss-type behaviour with a negative paramagnetic Curie temperature. The experimentally determined trend, in this case, is in agreement with the prediction of the spin fluctuation model [38]. The model is based on the concept of temperature induced moments for systems which have a strongly enhanced paramagnetic susceptibility or are weak ferromagnets, such as nickel in the present system. In the case of  $\text{LaNi}_5$ , the wavenumber dependent susceptibility has a large enhancement due to electron–electron interactions for small  $q$  values. The temperature dependence of  $\chi_q$  is significant only when  $q$  values are small. The average amplitude of the local spin fluctuations  $\langle S_{\text{loc}}^2 \rangle = 3k_{\text{B}}T \sum_q \chi_q$  is a temperature dependent quantity and increases with temperature until it reaches an upper limit determined by the charge neutrality condition, at a temperature  $T^*$ . The moments are localized in  $q$ -space. The spin fluctuations are saturated and the effective moment corresponds to given electron configuration only for a system which shows a strong exchange enhanced susceptibility, for example  $\text{YCo}_2$  or  $\text{LuCo}_2$  compounds having a high exchange enhanced (Stoner) factor [39]. For  $\text{LaNi}_5$ , the exchange enhancement factor is not so high and consequently the effective moment value seems to be nonsaturated. The determined effective Ni moment ( $2.15 \mu_{\text{B}}/\text{atom}$ ) is smaller than the characteristic value for  $\text{Ni}^{2+}$  ions considering only the spin contribution ( $2.83 \mu_{\text{B}}/\text{atom}$ ). For compounds with  $x \geq 0.2$ , nickel shows, at low temperatures, a weak ferromagnetism. Thus, the presence of effective nickel moments in the paramagnetic range may be also considered in the spin fluctuation model. The effective nickel moments decrease when increasing gadolinium content and exchange interactions, respectively. This behaviour may be ascribed to gradual quenching of spin fluctuations by internal fields.

The matter of quenching of spin fluctuations by external field was theoretically analysed [40–42]. According to Brinkman and Engelsberg [41] a magnetic field,  $H_{\text{eff}}$ , of the order of the characteristic spin fluctuation temperature,  $T_s$ , is required to quench spin fluctuation enhancement. The effective field is given by  $H_{\text{eff}} = k_{\text{B}}T_s/\mu_{\text{B}}s^{1/2}$ . If the magnetic field is sufficiently large so that the Zeeman splitting energy of opposite spin states is comparable to or larger than the characteristic spin fluctuation energy, then the paramagnet no longer has sufficient energy to flip spins and therefore the inelastic spin-flip scattering is quenched. Beal-Monod [40] showed that the decrease in heat capacity, at 0 K, for a nearly ferromagnetic Fermi liquid is proportional to  $H^2$ . Hertel *et al* [42] reported that the electronic contribution to the heat capacity would be depressed by a few percent, at 0.1 MOe, if the Stoner enhancement and the mass enhanced due to spin fluctuations are large and also if the spin fluctuation temperature is small. Experimentally, there has been shown in a field of 0.1 MOe a reduction of the electronic specific heat coefficient by 4% and 10% in strongly exchange enhanced paramagnets  $\text{YCo}_2$  and  $\text{LuCo}_2$ , respectively [43]. The analysis of our experimental data in the above models



shows a better agreement with the model of Hertel *et al* [42], although the agreement with  $H^2$  dependence [40] was also good.

Previously [44, 45], we showed that by increasing the exchange fields acting on Co in  $\text{RCO}_2$  compounds, when replacing non magnetic Lu by magnetic rare-earths, there is a decrease of the effective cobalt moment along the series from  $3.86 \mu_{\text{B}}$ /atom in  $\text{LuCo}_2$  or  $\text{YCo}_2$  up to  $2.60 \mu_{\text{B}}$ /atom in  $\text{GdCo}_2$ . This behaviour was attributed to partial quenching of spin fluctuations by internal fields. The effective cobalt moments vary linearly with the reciprocal of the exchange field. A decrease of 6% for the effective cobalt moments, in the above series, was shown when the internal field increased by 0.1 MOe. The above data may compare with nearly the same decrease in the electronic specific heat coefficient in nonmagnetic compounds of the  $\text{RCO}_2$  series ( $\text{R} = \text{Y}, \text{Lu}$ ) [43]. The effective nickel moments in  $\text{Gd}_x\text{La}_{1-x}\text{Ni}_5$ , as in  $\text{RCO}_2$  systems, vary linearly with the reciprocal of exchange field,  $M_{\text{eff}}(\text{Ni}) = 0.35 H_{\text{exch}}^{-1} \mu_{\text{B}}$ , where  $H_{\text{exch}}$  is given in MOe. We also evaluated an effective field required to quench the spin fluctuations as suggested by [40]. This is of the order of 0.8 MOe, in rather good agreement with the above experimentally observed dependence.

We note the great variation of the effective nickel moments in the composition range  $0 < x < 0.2$ . There is also a diminution of the paramagnetic Curie temperature (in absolute magnitude) from  $-1104 \text{ K}$  to the asymptotic value of  $-45 \text{ K}$  ( $x = 0.2$ ). These changes may be attributed to the transition from a system in which the magnetic properties are dominated, at  $x = 0$ , by spin fluctuations to one in which, for  $x = 0.2$ , the ferrimagnetic ordering is important.

Finally, we conclude that in the  $\text{Gd}_x\text{La}_{1-x}\text{Ni}_5$ , system there is a transition from spin fluctuation behaviour, characteristic for  $\text{LaNi}_5$ , to a ferrimagnetic type ordering for  $x > 0.2$ . The nickel moments, at 1.7 K, above a critical field, increase almost linearly with the exchange fields. The same trend was shown for mean nickel moments obtained from band structure calculations, these being little higher than those determined from magnetic measurements. The 4f–3d exchange interactions are mediated by the R 5d band. The Gd 5d band polarization is due both to local 4f–5d exchange and 5d–3d and 5d–5d band hybridizations by short range exchange interactions with neighbouring atoms. The mean effective nickel moments decrease when increasing gadolinium content, an opposite behaviour to that shown for Ni moments determined at 1.7 K. The magnetic behaviour of nickel seems to be best described in the spin fluctuation model. The decrease of the effective nickel moments was connected to gradual quenching of spin fluctuations by internal field, as the gadolinium content and exchange interactions respectively increase.

## References

- [1] Burzo E, Chelkovski A and Kirchmayr H R 1990 *Landolt Börnstein Handbook* vol III/19f2 (Berlin: Springer)
- [2] Burzo E 1981 *J. Less Common Met.* **77** 251
- [3] Burzo E, Plugaru N, Creanga I and Ursu M 1989 *J. Less-Common Met.* **155** 281
- [4] Duc N H, Tien T D, Brommer P E and Franse J J M 1992 *J. Magn. Magn. Mater.* **104–107** 1252
- [5] Burzo E 1995 *J. Magn. Magn. Mater.* **140–144** 973
- [6] Gignoux D, Givord D and del Moral A 1976 *Solid State Commun.* **19** 891
- [7] Buschow K H J 1971 *Phys. Status Solidi a* **7** 199
- [8] Wallace W E and Swearingen J T 1973 *J. Solid State Chem.* **8** 37  
Wallace W E, Ganapathy E V and Craig R S 1979 *J. Appl. Phys.* **50** 2327
- [9] Campbell I A 1972 *J. Phys. F: Met. Phys.* **2** L147
- [10] Riedli P C and Webber G D 1983 *J. Phys. F: Met. Phys.* **13** 1057  
Riedli P C, Dumelow T and Abel JS 1985 *Physica B* **130** 449  
Dumelow T, Riedli P C, Mohn P, Schwartz K and Yamada Y 1985 *J. Magn. Magn. Mater.* **54–57** 1089
- [11] Krén E, Schweizer J and Tasset F 1969 *Phys. Rev.* **186** 479  
Kennedy S J, Brown P J and Coles B R 1993 *J. Phys.: Condens. Matter* **5** 5169

- [12] Isnard O, Margalia S, Fruchart D, Giorgetti C, Pizzini S, Dartyge F, Kill G and Kappler L P 1994 *Phys. Rev. B* **49** 15962
- [13] Brooks M S S and Johansson B 1993 *Handbook of Magnetic Materials* vol 7 (Amsterdam: North Holland) p 139
- [14] Brooks M S S, Erikson O and Johansson B 1991 *J. Phys.: Condens. Matter* **3** 2357 and 3393  
Brooks M S S, Erikson O and Johansson B 1991 *Physica B* **172** 95
- [15] Brooks M S S, Gasche T, Auluck S, Nodström L, Severin L, Tryggvad J and Johansson B 1991 *J. Appl. Phys.* **70** 5972
- [16] Li H S, Li Y P and Coey J M D 1991 *J. Phys.: Condens. Matter* **3** 7227
- [17] Fähnle M 1993 *J. Magn. Magn. Mater.* **124** 239
- [18] Richter M 1998 *J. Phys. D: Appl. Phys.* **31** 1017
- [19] Jepsen O and Andersen O K 1995 *Z. Phys. B* **97** 35
- [20] Burzo E, Costina I and Chioncel L 2001 *Mater. Sci. Forum* **373–376** 669
- [21] Battes L F 1951 *Modern Magnetism* (Cambridge: Cambridge University Press) p 139
- [22] Andersen O K 1975 *Phys. Rev. B* **12** 3060
- [23] Andersen O K and Jepsen O 1984 *Phys. Rev. Lett.* **53** 2571
- [24] Andersen O K, Jepsen O and Glötzel D 1985 *Highlights of Condensed-Matter Theory* ed F Bassani, F Fumi and M P Tosi (Amsterdam: North-Holland) p 85
- [25] Jones R O and Gunnarson O 1989 *Rev. Mod. Phys.* **61** 689
- [26] Von Barth U and Hedin L 1972 *J. Phys. C: Solid State Phys.* **5** 1629
- [27] Pirogov A N, Kelarev V V, Ermolenko A S, Chuev V V, Sidorov S N and Artmanova A M 1982 *Zh. Exp. Teor. Fiz.* **583** 1398
- [28] Burzo E and Chioncel L 2004 *J. Opt. Adv. Mater.* **6** 917
- [29] Burzo E, Crainic T, Neumann M, Chioncel L and Lazar C 2005 *J. Magn. Magn. Mater.* **290/291** 371
- [30] Burzo E, Chiuzbăian S G, Chioncel L and Neumann M 2000 *J. Phys.: Condens. Matter* **12** 5897
- [31] Béal Monod M T 1982 *Physica B* **109/110** 1837
- [32] Fletcher G C 1971 *The Electron Band Theory of Solids* (Amsterdam: North Holland)
- [33] Anisimov V I, Aryasetiawan F and Lichtenstein A I 1997 *J. Phys.: Condens. Matter* **9** 767
- [34] Lichtenstein A I, Katsnelson M I, Antropov V A and Gubanov V A 1987 *J. Magn. Magn. Mater.* **67** 65
- [35] Neel L 1948 *Ann. Phys.* **3** 137
- [36] Burzo E and Laforest J 1972 *Int. J. Magn.* **3** 161
- [37] Burzo E 1972 *Solid State Commun.* **20** 569
- [38] Moriya T 1979 *J. Magn. Magn. Mater.* **14** 1  
Moriya T 1991 *J. Magn. Magn. Mater.* **100** 201
- [39] Burzo E, Gratz E and Pop V 1993 *J. Magn. Magn. Mater.* **123** 159
- [40] Béal Monod M T, Ma S K and Fredkin D R 1968 *Phys. Rev. Lett.* **20** 929
- [41] Brinkman W F and Engelsberg S 1968 *Phys. Rev.* **169** 417
- [42] Hertel P, Appel J and Fay D 1980 *Phys. Rev. B* **22** 534
- [43] Ikeda K, Gschneidner K A, Tsang R J E and Mc Masters O D 1989 *Phys. Rev. B* **29** 5039
- [44] Burzo E and Lemaire R 1992 *Solid State Commun.* **84** 1145
- [45] Burzo E 1997 *Balkan Phys. Lett.* **4** 208